Carbohydrate Polymers 106 (2014) 283–292

Contents lists available at ScienceDirect

Carbohydrate Polymers

journal homepage: www.elsevier.com/locate/carbpol

Modifying the flocculation of microfibrillated cellulose suspensions by soluble polysaccharides under conditions unfavorable to adsorption

Anni Sorvari[a], Tapio Saarinen[a], Sanna Haavisto[b], Juha Salmela[b], Maija Vuoriluoto[c], Jukka Seppälä[a,*]

[a] Polymer Technology, Department of Biotechnology and Chemical Technology, Aalto University, P.O. Box 16100, FI-00076 Aalto, Finland
[b] VTT Technical Research Centre of Finland, P.O. Box 1603, 40101 Jyväskylä, Finland
[c] Forest Products Surface Chemistry, Department of Forest Product Technology, Aalto University, P.O. Box 16300, 00076 Aalto, Finland

ARTICLE INFO

Article history:
Received 2 December 2013
Received in revised form 30 January 2014
Accepted 9 February 2014
Available online 18 February 2014

Keywords:
Microfibrillated cellulose
Rotational rheometry
Dispersant
Optical coherence tomography
Xanthan gum
Carboxymethyl cellulose

ABSTRACT

Carboxymethylcellulose (CMC) and xanthan gum were studied as dispersants for microfibrillated cellulose (MFC) suspension using a rotational rheometer and imaging methods. The imaging was a combination of photography and optical coherence tomography (OCT). Both polymers dispersed MFC fibers, although CMC was more effective than xanthan gum. The negatively charged polymer chains increased the viscosity of the suspending medium and acted as buffers in between the negatively charged fibers. This behavior decreased the number and strength of contacts between the fibers and subsequently dispersed the flocs. The stronger separation of the fibers was reflected in the frequency sweep where the MFC/polymer suspensions had lower gel strength than pure MFC suspension. Dispersing effect was also observed in the flow measurements, where the floc size was more uniform with polymers in the decelerating flow and after long, slow constant shear, which normally induces a heterogeneous structure with large flocs into the MFC suspension.

1. Introduction

Being a renewable raw material, wood and other cellulose resources are under constant investigations for new applications. Wood pulp can be disintegrated by mechanical shearing to microfibrillated cellulose (MFC) fibers, which have nanoscale diameters and length of several micrometers (Vartiainen et al., 2011). It is a potentially new material, for example, in nanocomposites (Nguyen et al., 2011; Svagan, Samir, & Berglund, 2007; H. Yano & Nakahara, 2004; H. Yano et al., 2005), paper making (Ahola, Österberg, & Laine, 2008; Eriksen, Syverud, & Gregersen, 2008), and as a rheology modifier (Turbak, Snyder, & Sandberg, 1983). As a rheology modifier, MFC has interesting properties in water suspensions, for example, gel formation at a very low concentration (~0.1%), thixotropy, and shear thinning behavior (Agoda-Tandjawa et al., 2010; Iotti, Gregersen, Moe, & Lenes, 2011; Karppinen et al., 2012; Pääkkö et al., 2007). These properties derive primaly from the inherent entangled network that forms when the fibers disintegrate to fibrils. A high fiber aspect ratio and partially disintegrated fibers strengthen the network within these suspensions (Pääkkö et al., 2007).

MFC suspensions, similar to many other fiber suspensions with a high aspect ratio, tend to form flocs when dispersed in water, unless specifically treated to prevent it. However, good dispersion and non-flocculated structure are required in many applications, for instance, transparent or high mechanical strength nanocomposites. Different means, for example, increasing the surface charge of the fiber (Saito, Nishiyama, Putaux, Vignon, & Isogai, 2006) or adding dispersants (Myllytie, Holappa, Paltakari, & Laine, 2009) may be used to disrupt the flocs and achieve better dispersion. The origin of the MFC flocs is both mechanical and colloidal (Hubbe & Rojas, 2008). MFC fibers are flexible and long compared to their diameter, which enhances mechanical flocculation, as is known for pulp fibers (R.J. Kerekes, 2006; R.J. Kerekes, Soszynski, & Tam Doo, 1985). This can occur via hooking of the fibers or the fibers can bend in flowing suspension, and during decelerating flow, become strained between other fibers, forming a three dimensional network. The frictional forces between the fibers are important factors in this mechanism. As MFC fibers are smaller than pulp fibers, in the colloidal scale, the colloidal forces are also important in flocculation. DLVO theory (Derjaguin & Landau, 1941; Verwey & Overbeek, 1948) is often used to describe the effect of van der Waals and

* Corresponding author. Tel.: +358 9 4702 2614; fax: +358 9 462 373.
E-mail addresses: anni.sorvari@aalto.fi (A. Sorvari), tapio.saarinen@aalto.fi (T. Saarinen), sanna.haavisto@vtt.fi (S. Haavisto), juha.salmela@aalto.fi (J. Salmela), maija.vuoriluoto@aalto.fi (M. Vuoriluoto), jukka.seppala@aalto.fi (J. Seppälä).

http://dx.doi.org/10.1016/j.carbpol.2014.02.032
0144-8617/

electrostatic double layer interactions. Van der Waals forces arise from the interactions between permanent, induced, or transient electronic dipoles (Hubbe & Rojas, 2008), which display attraction between similar surfaces. The electrostatic double layer is caused by ions that accumulate close to the charged surface; these layers create repulsion between like-charged surfaces. The thickness of the electrostatic double layer is dependent on the electrolyte concentration; the higher the ionic strength, the thinner the electrostatic double layer is.

MFC fibers can also have non-DLVO interactions, such as steric and electrosteric interactions, in the presence of polymers or polyelectrolytes in the system. The effect of polymers on flocculation and rheology of pulp suspensions has interested researchers, as many polymers are used in paper making as, for instance, retention aids to retain fines and fillers on the fibers (Stenius, 2000). These polymers can be anionic, cationic or neutral. The molecular weight and charge density of the ionic polymers are the most characteristic properties of the deflocculants (Gregory & Barany, 2011). Often, adsorption of the polymer is needed and the interactions causing that may be electrostatic interactions, hydrogen bonding, hydrophobic interactions, or ion binding (Gregory & Barany, 2011). If a high amount of a polymer is adsorbed on the fibers, the polymer can sterically stabilize the system. This is normally achieved with highly cationic polymers (Gregory & Barany, 2011). Some polymers, such as gums and mucilages (de Roos, 1958) and carboxymethyl cellulose (Laine, Lindström, Nordmark, & Risinger, 2000), are known to adsorb on cellulosic fibers, thus reducing the fiber–fiber friction, and in turn, mechanical flocculation.

Adsorption is not always necessary for the dispersing effect of polymers. High molecular mass anionic polymers can be used as dispersants for pulp and MFC, even if they do not adsorb on cellulosic surfaces at low electrolyte concentration. They can deflocculate the suspension by changing the shear or elongational viscosity of the suspending medium. An increased shear or elongation viscosity of the suspending medium reduces the turbulence intensity and the velocity of the approaching fibers, thus diminishing flocculation (R.J. Kerekes, 2006; Lee & Lindström, 1989; Yan, Lindström, & Christiernin, 2006; Zhao & Kerekes, 1993).

In this study, we utilized two commonly known anionic polysaccharides, carboxymethylcellulose (CMC) and xanthan gum, for controlling the flocculation and rheology of MFC suspensions. CMC is an anionic, linear cellulose derivative which is known to adsorb on cellulosic fibers in certain conditions, although the fibers and polymer are both negatively charged (Laine et al., 2000). Adsorption can be expected at high temperatures, long adsorption time, and sufficiently high salt concentration. CMC is known to deflocculate pulp suspensions (Beghello, 1998; Giri, Simonsen, & Rochefort, 2000; Horvath & Lindström, 2007; Liimatainen, Haavisto, Haapala, & Niinimäki, 2009; Yan et al., 2006). The dispersion effect has been attributed to the ability of CMC to lower the frictional forces between the cellulosic fibers (Yan et al., 2006; Zauscher & Klingenberg, 2000, 2001) if it is adsorbed onto the fibers. Some researchers have also discovered that CMC can disperse pulp without adsorbing on the fibers. The proposed mechanism involves CMC forming a non-adsorbed layer near the fiber surfaces, thus reducing fiber-to-fiber friction due to the large physical size of the CMC molecules (Liimatainen et al., 2009), or that anionic CMC molecules creates repulsive forces between the fibers and thus prevents flocculation (Rantanen, Molarius, Pikkarainen, Knuutinen, & Pakarinen, 2006).

The other polymer used here is a negatively charged xanthan gum which is less studied as a dispersant for pulp or MFC than CMC. It is used in the food industry as a stabilizer and thickener, because it has high viscosity at low concentration and is shear-thinning with yield stress and it is non-toxic (Ahmed & Ramaswamy, 2004). Xanthan gum is produced by the bacterium *Xanthomonas campestris*. The main chain is composed of a 1–4 linked β-D-glucose units with trisaccharide side chains. Some of the side chains carry acetic and pyruvic acid groups which make the polymer anionic (García-Ochoa, Santos, Casas, & Gómez, 2000). Under certain temperature and salt concentration, xanthan gum backbone undergoes an order-to-disorder (or helix-to-coil) transition which is also reflected in the rheological properties (Norton & Goodall, 1984; Rochefort & Middleman, 1987). In distilled water and at room temperature, the backbone is disordered and highly extended due to the negative side chains which repel each other. The extended chains may align and associate via hydrogen bonding and form a weakly associated structure. With salt, the backbone takes a helical structure with the charged side chains inside the helix. In this conformation, the molecules align easily and are strongly associated resulting in gel-like structure (Rochefort & Middleman, 1987).

Previously (Saarinen, Haavisto, Sorvari, Salmela, & Seppälä, 2014), a novel method was introduced to investigate the rheology of a fiber suspension together with the information of its structure and flow profile inside the suspension using a combination of a rotational rheometer and optical coherence tomography (OCT). In this paper, the same system will be utilized to study MFC flocculation with polymers. The two polymers, CMC and xanthan gum, were studied as a rheology modifier and deflocculant for MFC. First, the adsorption of CMC and xanthan gum on MFC model surface by a quartz crystal microbalance with dissipation (QCM-D) and the rheology of the polymer solutions as such will be shown. This will be followed by measurements performed using a dynamic rotational rheometer with a normal digital camera and optical coherence tomography (OCT) device to study the MFC/polymer suspensions. With these methods, the ability of the polymers to change the flocculation and interactions between the MFC fibers under flow were studied, not only from outer surface of the rheometer geometry, but also inside the suspension.

2. Experimental

2.1. Materials

Microfibrillated cellulose (UPM Fibril Cellulose) was obtained from UPM-Kymmene Corporation. The material was prepared from never-dried bleached kraft birch pulp by mechanical disintegration. The pulp was changed to its sodium form and washed with deionized water to an electrical conductivity less than 10 μS/cm according to a procedure introduced by Swerin, Ödberg, and Lindström (1990) and subsequently ground three times in Supermasscolloider (Masuko Sangyo, Japan). The MFC was received, washed and ground and its initial solid content was 2% (w/w). The fiber diameters of similarly prepared MFC have been measured to be between 10 and 30 nm with some larger fibril aggregates (Vartiainen et al., 2011). Polymers were carboxymethylcellulose (CMC) from Sigma–Aldrich (M_w 700,000 g/mol, degree of substitution (DS) 0.9, sodium salt) and xanthan gum from CP Kelco (Kelzan XG, mesh size 381 μm). The charge of xanthan gum was determined to be approximately 1.6 meq/g by conductometric titration with cationic polydiallyldimethylammonium chloride. Both polymers were used without purification.

The polymers were dissolved in Milli-Q water (electrical conductivity <0.2 μS/cm at 25 °C) at room temperature and mixed with a magnetic stirrer for at least 2 h. The MFC suspensions were diluted with Milli-Q water and combined with polymer solutions using two different polymer concentrations, shown in Table 1. The suspensions were mixed with a Heidolph RZR 2051 control propeller mixer at 1400 rpm for 10 min. The diameters of the propeller and beaker

Table 1
Electrical conductivity and pH of the suspensions at room temperature. Concentrations are given in mass percentage.

Suspension	pH	Conductivity (μS/cm)
MFC 0.5%	6.18	20
MFC 0.5% + CMC 0.05%	6.85	146
MFC 0.5% + CMC 0.11%	6.94	278
MFC 0.5% + xanthan gum 0.05%	5.69	80
MFC 0.5% + xanthan gum 0.11%	5.66	139

were 58 mm and 66 mm, respectively. The electrical conductivity and pH of the suspensions are listed in Table 1.

Nanofibrillated cellulose (NFC) for the model films was produced by first passing bleached birch pulp through a Masuko grinder three times, after which it was further homogenized with twenty passes through a M110P fluidizer (Microfluidics corp., Newton, MA, USA). Deionized water that was further purified with a Millipore Synergy UV unit was used in all experiments (MilliQ-water). NFC model surfaces were prepared according to the method described by (Ahola, Myllytie, Österberg, Teerinen, & Laine, 2008). The NFC gel was diluted to 0.190 wt% and ultrasonicated for 10 min at 25% amplitude setting and consecutively centrifuged at 10,400 rpm for 45 min. The nanofibrils were obtained from the resultant clear supernatant. This material is called nanofibrillated cellulose (NFC) to distinguish it from the coarser but otherwise similar material, MFC, used in the rheological characterization. The nanofibrils were spin-coated (Model WS-650SX-6NPP, Laurell Technologies, PA, USA) onto silica-coated QCM-D quartz crystals (Q-Sense) with a pre-adsorbed thin layer of polyethyleneimine (PEI) at 3000 rpm with 90 s spinning time. The crystals were stored at ambient conditions and were allowed to stabilize overnight in water prior to measurements with QCM-D.

2.2. Adsorption studies

Quartz Crystal Microblance with Dissipation (QCM-D) was used to monitor xanthan gum and carboxymethyl cellulose adsorption on the NFC model films. The basis of the QCM-D technique is the acoustic oscillation of quartz crystal which can be measured to monitor adsorption events. The simultaneously measured dissipation (D) yields information about the viscoelastic properties of adsorbing layers (Höök, Rodahl, Brzezinski, & Kasemo, 1998; Rodahl, Hook, Krozer, Brzezinski, & Kasemo, 1995). The frequency and dissipation change are measured at a fundamental resonance frequency and its overtones.

The QCM-D measurements were performed using a Q-Sense E4 instrument (Västra Frölunda, Sweden). The adsorbed mass is proportinal to the change in resonance frequency according to the Sauerbrey equation (Eq. (1)) provided that the adsorbed layer is uniformly distributed on the surface, rigid and small compared to the crystal's mass (Rodahl & Kasemo, 1996; Sauerbrey, 1959):

$$\Delta m = \frac{C_{QCM-D}\Delta f}{n}, \quad (1)$$

where C_{QCM-D} is 0.177 mg Hz^{-1} m^{-2} for 5 MHz crystal (provided by the manufacturer), Δf is the change in frequency and n is an overtone number. The QCM-D measurements were conducted with a 0.1 ml/min constant flow rate at 23 °C. Each QCM-D measurement was performed three times. Results are calculated from the 3rd overtones.

Xanthan gum and CMC (0.1 mg/ml) in water were allowed to adsorb on NFC surfaces after first acquiring a stable baseline with water. Rinsing with water was applied when adsorption plateau was indicated by the QCM-D signals to study the irreversibility of the binding of given molecules on the NFC surfaces.

2.3. Rheological measurements

The measurements were performed using a dynamic rotational rheometer (ARG2, TA Instruments), with a metal concentric cylinders geometry (bob and cup radii 14.00 and 15.19 mm) fulfilling the standard ISO 3219/DIN 53 019. After a 20 min preshear interval at apparent 250 s^{-1} and a subsequent 10 min recovery period (time sweep at 0.5% strain and 1 Hz frequency), the frequency sweep was measured from 0.02 to 200 rad/s at 0.5% strain and amplitude sweep from the strain 0.01–1000% at a frequency of 1 Hz. The flow curve was measured strain controlled from apparent shear rates 500 (MFC) or 300 (suspensions with polymers) to 0.1 s^{-1} with a point time of 15 s. In addition, the suspensions were sheared at two apparent shear rates (500 and 0.5 s^{-1}) for 10 min. After each shear rate, a 10 min time sweep was measured at 0.5% strain and 1 Hz frequency.

2.4. Imaging

A tailor-made transparent polymethylmethacrylate (PMMA) outer geometry (radius 14.87 mm) was used in order to photograph the changes in suspension structure during the measurements. The cup was placed into a transparent water container to prevent reflections. The photographs were taken with Nikon D90 (Nikon Corporation, Japan) camera controlled by NKRemote software (Breeze Systems Limited, UK). Simultaneously, the suspension was recorded with optical coherence tomography. The method is described in detail in Saarinen et al. (2014). The device was a Spectral Domain OCT (Telesto SD-OCT, Thorlabs Inc.) with a central wavelength of 1325 nm. In the SD-OCT, a light beam of low coherence is emitted from a super luminescent led light source and split into the sample arm and the reference arm of the Michelson interferometer. The backscattered interference pattern carries information about the sample scattering index from different depths. Slice images are constructed from a series of adjacent lateral scans. In Doppler OCT mode, the velocity data is acquired using Kasai autocorrelation function of adjacent scans (Kasai, Namekawa, Koyano, & Omoto, 1985).

The device was set to acquire 2D slice images consisting of 500 radial scans across a lateral width of 1 mm. The resolution and frame rate of the slice images are determined by the light beam properties (central wavelength, coherence length and dimensions) and the radial scan rate. With the current device the radial resolution in water was approximately 5 μm and the lateral resolution was 15 μm. Three discrete values, 5.5, 28 and 91 kHz, were available for the radial scan rate. The value was selected based on the shear rate, aiming to minimize the structure motion between two sequential slice images which is detrimental for image quality. At the highest radial scan rate, a mean frame rate of 12 ms was achieved.

A sequence of 2D images was recorded at each shear rate during the stepped flow measurements. In addition to structural characterization, the images were utilized to determine the radial mean velocity profile by tracking the horizontal displacement of the MFC flocs between sequential structure images. The tracking was realized with an optical flow algorithm developed for fiber flocculation studies (Salmela & Kataja, 2005). The presented experimental setup allowed structure motion to be tracked over shear rates from 0.1 to approximately 50 s^{-1} in the vicinity of the outer cylinder wall. The velocity profiles could be built up over shear rate range of 0.1 to approximately 15 s^{-1}. Above that, the profile span was limited by the image quality near the inner cylinder.

Table 2
Adsorbed mass of xanthan gum and CMC on NFC model surface after 58 min adsorption and after 60 min adsorption and 10 min rinsing period calculated from the 3rd overtone by Eq. (1). Three parallel samples were measured and the error was calculated by standard deviation.

Polymer	Adsorbed amount (mg/m^2)	Adsorbed amount after rinsing (mg/m^2)
Xanthan gum	0.6 ± 0.3	0.4 ± 0.3
CMC	0.1 ± 0.4	0.0 ± 0.4

3. Results and discussion

3.1. Adsorption of CMC and xanthan gum on the NFC model surface

The adsorption of the polymers onto the fibers is one of the mechanisms how the polymers can prevent flocculation of pulp (Beghello, 1998; Giri et al., 2000; Watanabe, Gondo, & Kitao, 2004; Zauscher & Klingenberg, 2001). Therefore, the adsorption of CMC and xanthan gum on the MFC fibers was studied by using QCM-D and NFC model films. Since the model films were made from a similar pulp as the MFC used in this study, it is assumed that the NFC model film represents the MFC fiber surface and can be used to evaluate the adsorption of the polymers on the MFC fibers. The studies were performed in MilliQ water without any additional electrolytes to simulate the conditions used in the rheological measurements. The measurement was started by stabilizing the model surface in MilliQ water flow. After achieving a constant baseline, the flow of the polymer solutions to the surface was started. Table 2 shows the adsorbed mass after 58 min flow of polymer solution to the surface calculated by Eq. (1) from the third overtone of the frequency. After an one hour adsorption period, rinsing with MilliQ water was started and the adsorbed mass after 10 min of rinsing is also shown in Table 2. Both polymers showed minimal change in the adsorbed mass which even decreased when the rinsing was started. The results show that the conditions were not favorable for adsorption of the polymers to the NFC surface.

The observed increase in mass was almost negligible compared to adsorption which has been obtained for polysaccharides in more favorable conditions (P. Eronen, Junka, Laine, & Österberg, 2011; Junka et al., 2012; Orelma, Teerinen, Johansson, Holappa, & Laine, 2012). For instance, Orelma et al. (2012) measured 11 mg/m^2 adsorption of CMC on cellulose surface, when using 100 mM $CaCl_2$. In general, polysaccharides tend to adsorb onto cellulose surfaces due to the structural similarities of the polysaccharides and cellulose molecules (de Roos, 1958; Eronen et al., 2011; Myllytie, Salmi, & Laine, 2009). In particular, CMC has a high affinity toward cellulose surfaces (Laine et al., 2000). However, the negative charge of the polymers imped adsorption onto the NFC surface in electrolyte-free conditions (Junka et al., 2012). Moreover, the side chains of xanthan gum could prevent the close contact between the polymer backbones, thus preventing the adsorption (de Roos, 1958). Both polymers had fairly large molecular masses which may further decrease the adsorption. Applying these results to MFC/polymer suspensions, it can be concluded that CMC and xanthan gum do not significantly adsorb onto MFC fibers in electrolyte free-conditions.

3.2. Rheology of the polymer solutions

Fig. 1 shows the frequency sweeps and flow curves for CMC and xanthan gum solutions without MFC. At low frequencies, both solutions had higher loss modulus (G'') than storage modulus (G'). With increasing frequency the moduli increased; however, storage modulus increased more than loss modulus. At high frequencies, the storage modulus was higher than loss modulus for both polymer solutions. This is typical behavior for semi-dilute entangled polymer solutions, and it shows that the polymer chains were weakly associated in the solution but not strongly enough at this concentration to produce gel-like behavior across the whole frequency range (Rochefort & Middleman, 1987). Xanthan gum is disordered or partially disordered in electrolyte-free conditions but highly extended due to the electrostatic repulsion between the charged side chains. The xanthan gum chains can align and associate via hydrogen bonding to form weak structures (Rochefort & Middleman, 1987), which explains the moduli levels. CMC had relatively high molecular weight and degree of substitution, which causes extended chain conformation and repulsion between the polymers chains and resulted in the high moduli. The crossover point of the loss and storage moduli was approximately 1 rad/s for xanthan gum solution and approximately 100 rad/s for CMC solution. This indicates that xanthan gum chains had longer relaxation times than CMC solution which could mean that xanthan gum chains had longer-range interactions with each other than CMC molecules. In addition, xanthan gum had higher storage and loss modulus than CMC which was probably due to the stronger interactions between the xanthan gum polymer chains. The radius of gyration can be estimated to be approximately 100 nm for the CMC in these conditions (Gondo, Watanabe, Soma, & Kitao, 2006) which is lower than for xanthan gum based on the mesh size (381 nm), thus further explaining the higher moduli of the xanthan gum solution.

Flow curves for the polymer solutions in Fig. 1 show that both polymers were shear-thinning with Newtonian plateau at low shear rates. Shear-thinning behavior is in accordance with the trends observed in the frequency sweeps and shows that a loss of the ordered structure occurred during the flow measurement. Xanthan gum had higher viscosity at low shear rates but it was more shear-thinning than CMC solution, resulting in the lower viscosity of xanthan gum at high shear rates compared to CMC. This can be explained by the larger size distribution of xanthan gum or xanthan

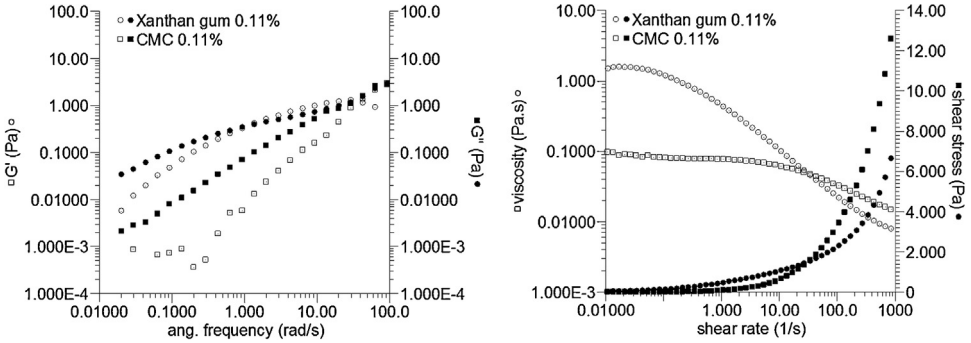

Fig. 1. Frequency sweeps and flow curves for the xanthan gum (circles) and CMC (squares) solutions.

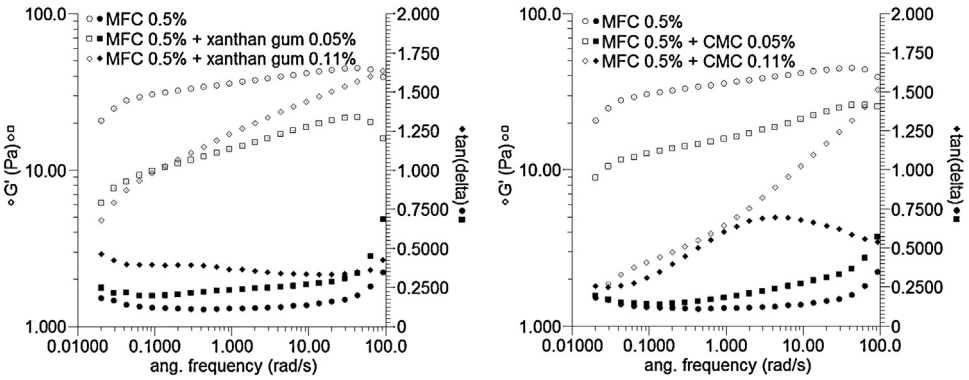

Fig. 2. Frequency sweeps for MFC suspension as such and with polymer additives.

gum solution was more structured and was able to align within the flow when shear rate was increased.

3.3. Effect of polymers on MFC suspension gel strength

Fig. 2 shows the frequency sweeps for the MFC suspensions with polymers. Frequency sweeps were measured within the linear viscoelastic region, as confirmed with the amplitude sweep measurements (results not shown). Fiber suspensions are prone to wall depletion, particularly in steady shear measurements. Therefore, oscillation measurements in the linear viscoelastic region were used as an indication of the gel strength, since the problems with wall depletion are expected to be diminished with small stresses and strains after a suitable pre-shear period (Barnes, 1995; Björkman, 2006; Buscall, 2010; Saarinen et al., 2014). Pure MFC suspension had a higher storage modulus than loss modulus, and the moduli were rather independent of angular frequency, indicating gel-like behavior. Adding either CMC or xanthan gum to the suspension decreased the storage modulus and increased the tan delta of the suspension compared to the pure MFC suspension. This shows that gel strength decreased and the suspension turned more fluid-like with CMC and xanthan gum addition, although the suspensions still behaved like gels. The lower amount of polymer (0.05%) decreased the storage modulus but the slope of the curve was almost the same as in the pure MFC suspension. At higher polymer concentrations (0.11%), xanthan gum lowered the storage modulus less than CMC, although both polymers increased tan delta and made the storage modulus clearly increase with frequency.

The storage modulus provides information about the strength of the fiber network at rest which is dependent on the strength of the average fiber–fiber contact and the number of contact points between the fibers (R.J. Kerekes et al., 1985). Earlier studies have shown that CMC lowers the yield stress (Beghello & Lindström, 1998; Horvath & Lindström, 2007) and moduli (Giri et al., 2000) of pulp suspensions and it has been connected to better dispersion of the pulp fibers. Lower moduli suggest that both polymers dispersed the MFC suspension and weakened the interactions between the fibers. The more liquid-like behavior (higher tan delta) observed with 0.11% polymer concentration also suggests that there were fewer or weaker contacts between the fibers. At 0.05% polymer concentration, both polymers decreased the gel strength similarly. At 0.11% polymer concentration, CMC lowered the storage modulus more than xanthan gum, suggesting that CMC dispersed the MFC fibers better than xanthan gum. CMC had a higher charge density which could explain its greater effect on the gel strength. Furthermore, xanthan gum solution had a higher gel storage modulus than CMC solution, as was shown in Fig. 1, which may be the reason for higher gel strength in MFC/xanthan gum suspensions compared to MFC/CMC suspensions.

3.4. Flow properties and floc structures

The ability of CMC and xanthan gum to prevent shear-induced flocculation of MFC was studied in a stepped flow measurement. In order to see the floc structure, the suspensions were measured in the transparent geometry with a rheometer, and the floc structure of the suspensions was observed with normal digital camera and optical coherence tomography (OCT). The transparent geometry consists of a standard metal inner cylinder (oxidized aluminum surface) and transparent polymethylmethacrylate (PMMA) outer cylinder. Flow curves for the suspensions with transparent cup are shown in Fig. 3. Although wall depletion impairs the rheological data obtained from the flow measurements (Saarinen et al., 2014), together with the imaging it gives information about the suspension structure in decelerating flow. Especially at low shear rates, the suspension slips at the geometry walls and flows as a plug flow. At higher shear rates (above the yield stress), the suspension is under shear but the velocity profile is not linear due to wall slip at both geometry walls (Saarinen et al., 2014). Therefore, the shear rates presented here must be considered as apparent ones. The suspensions were photographed and recorded with OCT at every shear rate, except the highest shear rates where the imaging was impossible (maximum shear rate for OCT imaging was approximately 10–20 s^{-1} and for photographs 100 s^{-1}). Figs. 4 and 5 show the suspension structure at certain shear rates recorded by camera and OCT. In addition, the OCT images contain the velocity profile calculated from the consecutive images in those cases when it was possible.

The measurement started from the high shear rates. Fig. 4c, f, and i shows the structure of the suspensions at the apparent

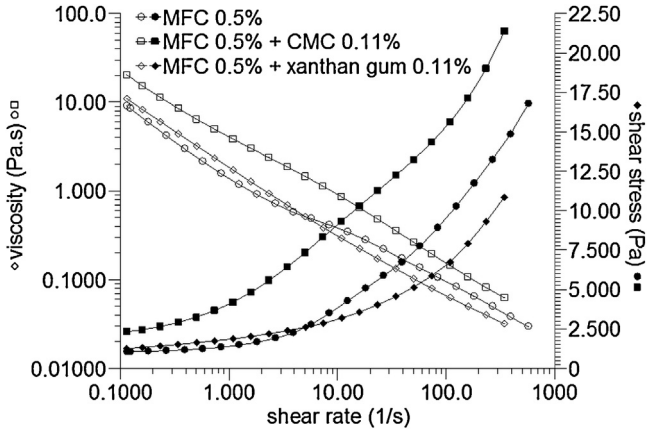

Fig. 3. Flow curves for MFC suspensions as such and with polymer additives measured with transparent cup.

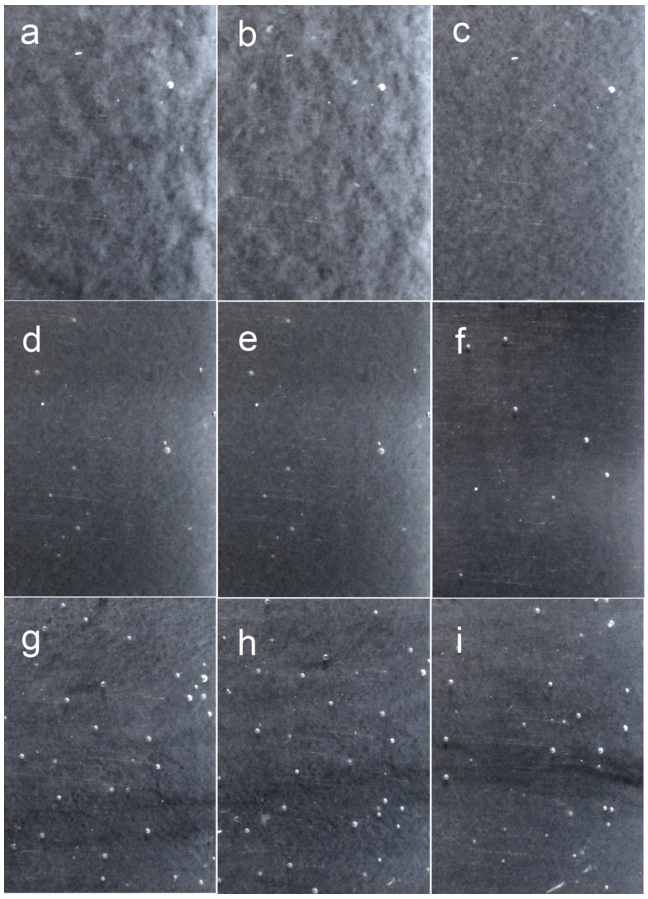

Fig. 4. Photographs from the suspensions at three apparent shear rates: 0.5% MFC suspension at apparent shear rate (a) 0.6 s^{-1}, (b) 6 s^{-1}, (c) 64 s^{-1} from the flow curve measurements. 0.5% MFC suspension with 0.11% CMC at apparent shear rate (d) 0.6 s^{-1}, (e) 6 s^{-1}, (f) 64 s^{-1}. 0.5% MFC suspension with 0.11% xanthan gum at apparent shear rate (g) 0.6 s^{-1}, (h) 6 s^{-1}, (i) 64 s^{-1}. The width of the photographed area is 10 mm.

shear rate 64 s^{-1}. At high shear rates, macroscopic floc structure consists of small and same-sized flocs, as we have shown earlier (Karppinen et al., 2012; Saarinen et al., 2014), and the polymers did not change this. At high shear rate region, the suspension is under shear, despite suffering from wall depletion at the outer wall (Saarinen et al., 2014). The viscosity and shear stress of the polymer containing suspensions differentiated the most from the pure MFC suspension in this region, see Fig. 3. The apparent viscosity is the sum of the polymers' effect on the MFC floc size and depletion layer. At high shear rates, the viscosity of the polymer solutions seemed to determine the apparent viscosity of the suspensions. CMC solution viscosity was higher than the viscosity of xanthan gum solution at high shear rate, and similarly MFC suspension with CMC had higher viscosity and shear stress than MFC suspension with xanthan gum. Both CMC and xanthan gum disperse the flocs, which lowers the shear stress at a given shear rate (Barnes, 1995), but in the case of CMC, the increased medium viscosity dominates the response.

At intermediate shear rate, flocs started to adhere to each other in the pure MFC suspension as the shear rate decreased, resulting in a very heterogeneous structure shown in Fig. 4b. Within this range, the slope of the shear stress decreased clearly. In the suspensions containing either xanthan gum or CMC, the fibers were more evenly distributed, and no clear change occurred in the floc structure (Fig. 4e and h). Moreover, the shear rate, where shear stress started to level as a function of shear rate, is clearly lower for the CMC suspension and higher for the xanthan gum suspension compared to pure MFC suspension. It is evident that floc adhesion in decelerating flow differs with polymers compared to the pure MFC suspension. The dispersing effect of the polymers prevents the floc size from changing, but the flocs still gradually attach to each other at their extremities.

The OCT images in Fig. 5 show the structure of the suspensions over the gap at intermediate and low shear rates. The pure MFC suspension showed flocs and water between them. The addition of CMC or xanthan gum resulted in a better dispersion in the suspension through the gap, although the structure appeared slightly more flocculated toward lower shear rates. This further confirms that both polymers dispersed the floc structure in decelerating flow compared to pure MFC. The velocity profiles in Fig. 5 show that pure MFC suspension (first row) slips at both geometry boundaries and flows as a plug flow, as we have reported earlier (Saarinen et al., 2014). For xanthan gum (third row in Fig. 5), the situation is similar, although it slips more at the inner cylinder compared to pure MFC. Instead, the suspension with CMC (the second row in Fig. 5) shows some deformation within the bulk at shear rate 5.7 s^{-1}, which further suggests that the forces between the flocs were weaker in the MFC/CMC suspension. Unfortunately, it was not possible to calculate the velocity profile for the higher shear rate due to the recording frequency in the MFC/CMC suspension being too low.

At the low shear rate end of the flow curve, both polymers slightly increased the shear stress of the MFC suspension. This is presumably from the increase in viscosity of the depleted layer. Within the low shear rate range, OCT results confirm that the suspension is not under shear but flows in a plug attached to the inner geometry surface except in the MFC/xanthan gum suspension where the bulk is attached to the outer cylinder wall. OCT images from a low shear rate, 0.5–0.6 s^{-1}, show that all suspensions slide at the geometry wall at this low shear rate region, and shear is concentrated to the depletion layer near the outer or inner boundary.

It seemed that the floc size was independent from the shear rate for suspensions with polymer addition, and the only change in the structure was that at high shear rate the flocs are detached from each other and rolled in the flow. It shows that the polymers prevented collisions between the fibers or reduced friction at fiber contact points; hence, the fibers remained dispersed and floc size small throughout the apparent shear rate range. Furthermore, OCT results show that wall depletion is present at all shear rates, and therefore, the shear rates and shear stresses must be considered as apparent ones.

3.5. Floc structure after constant shear

Both polymers, CMC and xanthan gum, had a very similar effect on the floc structure of MFC suspensions during the stepped flow measurement, where each shear rate was applied for 15 s. To investigate whether there was a difference between these two polymers at longer time scale, the suspensions were sheared for 10 min at two different shear rates, 0.5 and 500 s^{-1}, and the suspension structure was photographed immediately afterwards at rest. The structures are shown in Fig. 6. With pure MFC, the more homogeneous structure, the higher the preceding shear rate. Surprisingly, an opposite trend was observed for the polymer-containing suspensions. After low shear rate (0.5 s^{-1}), the suspensions with CMC and xanthan gum were well dispersed but after the 500 s^{-1} shear, the suspensions contained horizontal darker and lighter belts over the geometry height. Darker belts were visibly fiber free, while the fibers were packed in the lighter belts. Similar structures have earlier been observed for rodlike virus suspensions (Kang, Lettinga, Dogic, & Dhont, 2006), although their belts were smaller in scale and more regularly shaped. It has been suggested that the phenomenon is related to development of normal stresses toward the

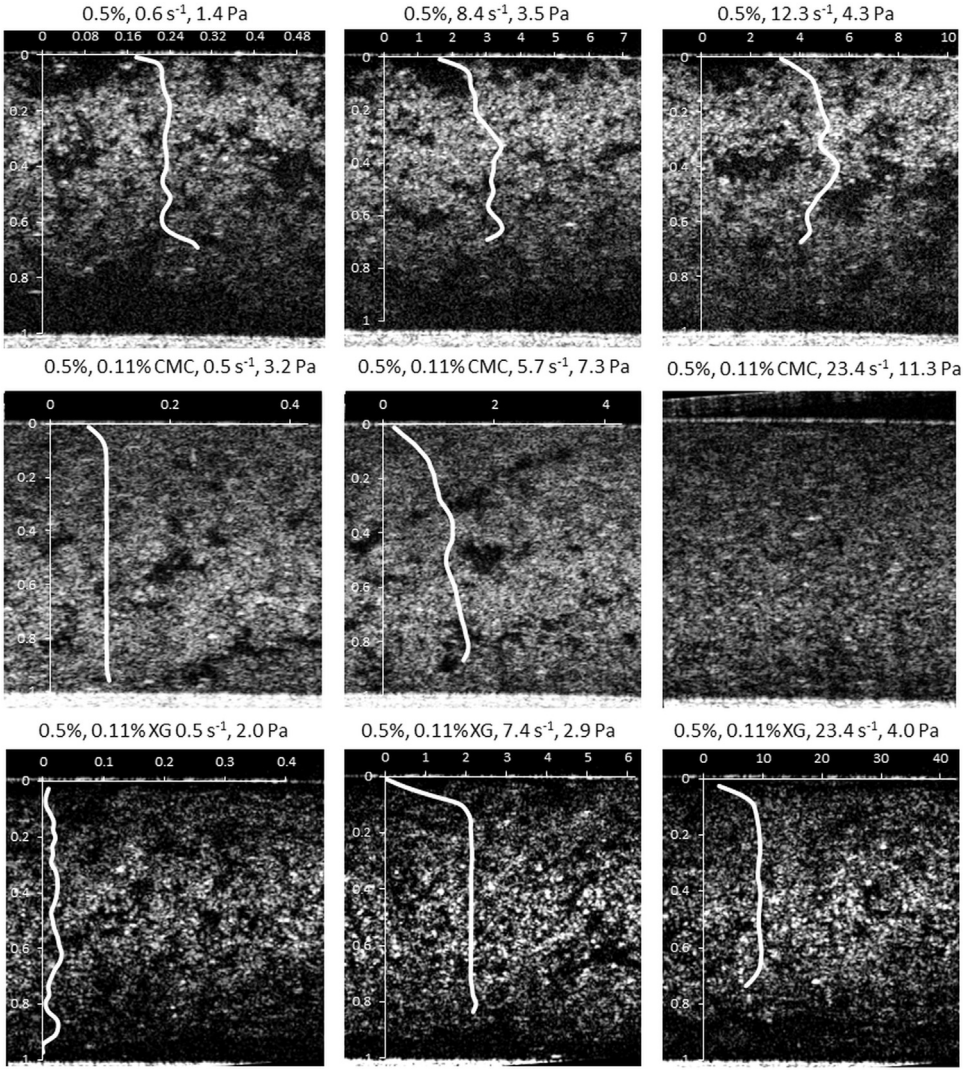

Fig. 5. OCT images from the suspensions at three different apparent shear rates. White lines indicate the velocity profile through the gap. *X* axis is velocity in mm/s and *y* axis distance from the outer geometry wall in mm. First row: 0.5% MFC suspension, second row: 0.5% MFC with 0.11% CMC, third row: 0.5% MFC with xanthan gum.

inner cylinder of the concentric cylinders geometry (Dhont & Briels, 2003). The inhomogeneties (in this case flocs or polymer chains) act like polymer chains in the Weissenberg effect (Weissenberg, 1947) causing normal stresses (Dhont & Briels, 2003; Kang et al., 2006). However, the belts were formed under such a high shear rate that it was not possible to observe the possible flows in the gap, and therefore, the mechanism behind the stripes remains unclear.

At low shear rates, the polymers dispersed MFC flocs. The apparent shear rate of 0.5 s^{-1} caused a very heterogeneous structure to MFC suspension (Fig. 6d), since the shear stress induced collisions between the fibers and thus mechanical flocculation. However, it was not sufficient to break flocs. Both polymers prevented this effectively as is shown in Fig. 6e and f. Qualitative inspection of the images of polymer-containing suspensions reveals that CMC addition resulted in a better dispersed structure than xanthan gum. This supports the conclusion made from the gel strength results (Fig. 2) where the MFC suspension with CMC showed lower moduli than MFC suspension with xanthan gum, and reduced interactions or decreased contacts between the fibers were expected to lead to this lower gel strength.

3.6. Discussion on dispersing mechanism of the polymers

MFC fibers form a three dimensional network where the junction points are partially disintegrated fibers or mechanical entanglements. The small negative surface charge (65 μeq/g (P. Eronen, Laine, Ruokolainen, & Österberg, 2012)), that the fibers have, causes slight repulsion between the fibers, thus preventing the aggregation to some extent. Under flow, the network is broken and new flocs can form mainly by mechanical hooking or bending and locking of the fibers in the flow (R.J. Kerekes et al., 1985). Imaging during flow curve measurements and after 10 min constant shear showed that both CMC and xanthan gum clearly dispersed shear-induced flocs in long, slow shearing. The better dispersed structure was also observed in frequency sweep where the suspensions with polymer had lower moduli than the pure MFC suspension. CMC has been studied widely as a dispersant for pulp fibers (de Roos, 1958; Giri et al., 2000; Liimatainen et al., 2009; Rantanen et al., 2006; Watanabe et al., 2004; Zauscher & Klingenberg, 2001) and MFC fibers (Myllytie, Holappa, et al., 2009; Myllytie, Salmi, et al., 2009). CMC's ability to disperse pulp has mainly been attributed to lowering the friction between the fibers

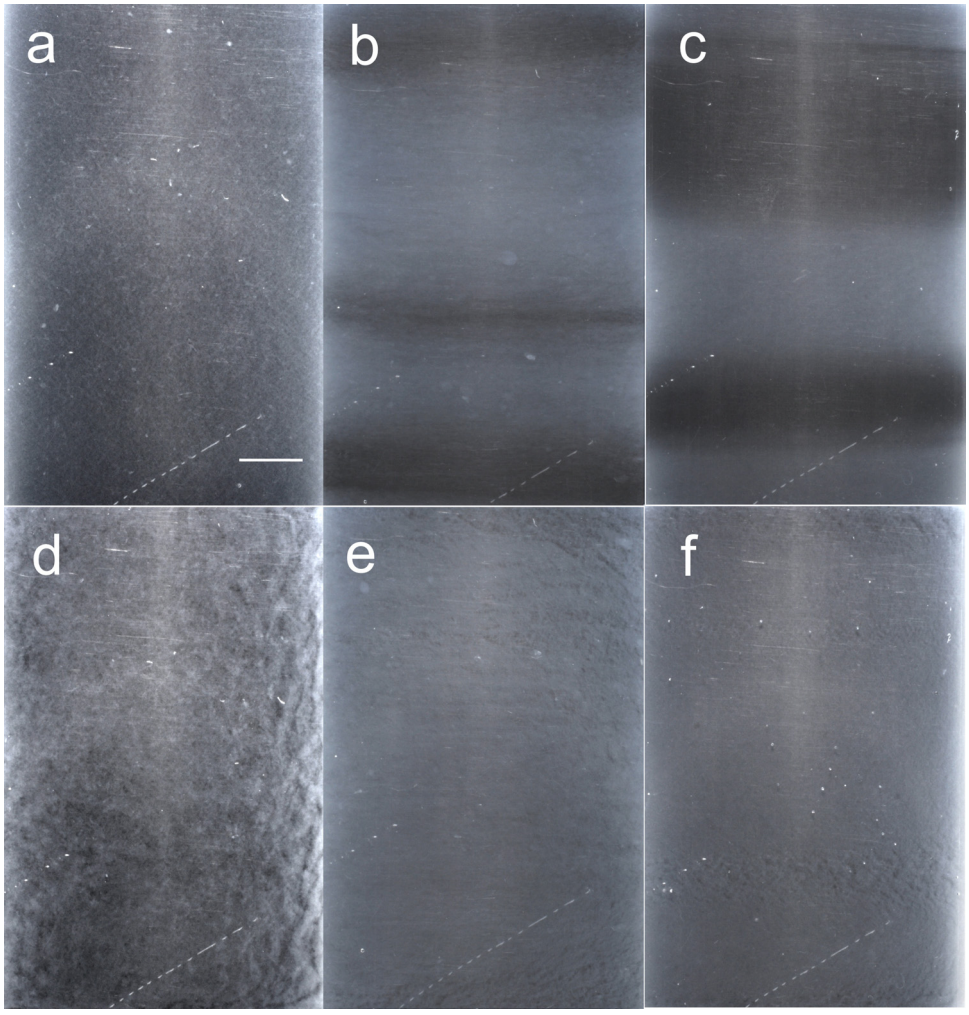

Fig. 6. Images of the MFC 0.5% suspensions after shearing at 500 (a–c) and 0.5 s^{-1} (d–f) for 10 min. (a and d) Pure MFC 0.5%, (b and e) with 0.11% xanthan gum, and (c and f) with 0.11% CMC. Scale bar represents 5 mm.

and thus preventing mechanical flocculation (de Roos, 1958; Giri et al., 2000; Watanabe et al., 2004; Zauscher & Klingenberg, 2001). This mechanism requires adsorption of the polymer onto the fibers. However, in this study, negligible amount of the polymers adsorbed onto the fibers, and therefore other mechanisms must be considered. Increased viscosity of the suspending medium has been shown to decrease mechanical flocculation (Soszynski & Kerekes, 1988; Yan et al., 2006; Zhao & Kerekes, 1993), since it reduces the relative motion of the fibers. The rheology of the suspending medium can also affect how much the fibers bend in the flow and thus how strained they are when they come to rest, and therefore higher viscosity should lead to higher capability to disperse fibers (Zhao & Kerekes, 1993). Xanthan gum had higher zero shear viscosity than CMC, however CMC resulted in more evenly distributed MFC fibers. This suggests that there are other factors than just viscosity affecting the dispersing ability of the polymer. The negative polymer chains between the fibers may have prevented collisions between the MFC fibers (Liimatainen et al., 2009; Rantanen et al., 2006). CMC had roughly three times higher charge density than xanthan gum which could explain the better dispersion. The structure of the polymers was also different, since CMC is linear and highly charged and thus in extended conformation. Xanthan gum was more structured and had intermolecular interactions based on the solution rheology, which has been related to diminished ability to disperse pulp fibers (de Roos, 1958; Svedberg, 2012). Using conditions favorable to adsorption of the polymers onto MFC could give more insights to the mechanisms of the dispersion effect.

4. Conclusions

CMC and xanthan gum were studied as dispersants for MFC suspension. Using OCT together with rotational rheometry, we were able to show how MFC fibers are dispersed by the two polymers in shear flow. Both polymers were negatively charged polysaccharides. CMC is linear and had higher charge density than xanthan gum, which is branched. Without additional salt, the polymers did not adsorb onto MFC fibers. The dispersing ability of the polymers was investigated by rheological characterization and visual observation of the floc structure over the shear rate range and during the 10 min constant shear. Stronger separation of the fibers was reflected in the frequency sweep where the MFC suspension with polymers had lower gel strength and more liquid-like behavior than the pure MFC suspension. Dispersing effect was also observed in the flow curve measurement where the floc size of the suspension was rather constant over the shear rates with polymers. This is different compared with MFC suspensions without any additives where the floc size is dependent on the shear rate. After a constant shear at low shear rate, the floc structure of the suspensions was clearly better dispersed in the suspensions with polymers, confirming the dispersing effect of the polymers.

This study showed that CMC and xanthan gum can be utilized to reduce shear induced flocculation of MFC suspensions. Moreover, it is not necessary to use polymer which adsorbs onto MFC fibers. CMC is known to disperse pulp and it was now confirmed that it disperses MFC fibers as well. Xanthan gum has not been studied as a dispersant for pulp. Both polymers decreased the number and strength of contacts between the fibers and thus decreased flocculation. The mechanism behind the enhanced dispersion of MFC fibers may include several aspects. First, both polymers increased the viscosity of the suspending medium, thus reducing the relative motion of the fibers. Second, the negatively charged polymer chains, in between the negatively charged fibers, may have prevented collisions and contacts between the fibers. CMC had better ability to disperse MFC based on the qualitative inspection of the suspension structure and lower gel strength measured in the oscillation measurement. This can be due to the higher charge density of CMC or smaller and more linear structure of CMC compared to xanthan gum.

This combination of a rotational rheometer with two imaging methods, optical camera and OCT, has proved to be an effective way of studying the dispersing ability of the polymers.

Acknowledgement

This work was a part of the Nanosellu III – project established by the Finnish Centre for Nanocellulosic Technologies. The project was funded by the Finnish Funding Agency for Technology and Innovation (Tekes). AS would like to acknowledge the Graduate School in Chemical Engineering for funding. Dr. Antti Laukkanen and Dr. Markus Nuopponen (UPM-Kymmene Oyj) are thanked for valuable discussions on MFC properties.

References

Agoda-Tandjawa, G., Durand, S., Berot, S., Blassel, C., Gaillard, C., Garnier, C., et al. (2010). Rheological characterization of microfibrillated cellulose suspensions after freezing. *Carbohydrate Polymers*, *80*(3), 677–686.

Ahmed, J., & Ramaswamy, H. S. (2004). Effect of high-hydrostatic pressure and concentration on rheological characteristics of xanthan gum. *Food Hydrocolloids*, *18*(3), 367–373.

Ahola, S., Myllytie, P., Österberg, M., Teerinen, T., & Laine, J. (2008). Effect of polymer adsorption on cellulose nanofibril water binding capacity and aggregation. *BioResources*, *3*(4), 1315–1328.

Ahola, S., Österberg, M., & Laine, J. (2008). Cellulose nanofibrils adsorption with poly(amideamine) epichlorohydrin studied by QCM-D and application as a paper strength additive. *Cellulose*, *15*(2), 303–314.

Barnes, H. A. (1995). A review of the slip (wall depletion) of polymer solutions, emulsions and particle suspensions in viscometers: Its cause, character, and cure. *Journal of Non-Newtonian Fluid Mechanics*, *56*(3), 221–251.

Beghello, L. (1998). Some factors that influence fiber flocculation. *Nordic Pulp & Paper Research Journal*, *13*(4), 274–279.

Beghello, L., & Lindström, T. (1998). The influence of carboxymethylation on the fiber flocculation process. *Nordic Pulp & Paper Research Journal*, *13*(4), 269–273.

Björkman, U. (2006). The metarheology of crowded fibre suspensions. *Annual Transactions of the Nordic Rheology Society*, *14*, 69–78.

Buscall, R. (2010). Letter to the editor: Wall slip in dispersion rheometry. *Journal of Rheology*, *54*(6), 1177–1183.

de Roos, A. J. (1958). Stabilization of fiber suspensions. *Tappi*, *41*(7), 354–358.

Derjaguin, B., & Landau, L. (1941). Theory of the stability of strongly charged lyophobic sols and of the adhesion of strongly charged particles in solutions of electrolytes. *Acta Physicochimica URSS*, *14*, 633–662.

Dhont, J. K. G., & Briels, W. J. (2003). Viscoelasticity of suspensions of long, rigid rods. *Colloids and Surfaces A: Physicochemical and Engineering Aspects*, *213*, 131–156.

Eriksen, O., Syverud, K., & Gregersen, O. (2008). The use of microfibrillated cellulose produced from kraft pulp as strength enhancer in TMP paper. *Nordic Pulp & Paper Research Journal*, *23*(3), 299–304.

Eronen, P., Junka, K., Laine, J., & Österberg, M. (2011). Interaction between water-soluble polysaccharides and native nanofibrillar cellulose thin films. *BioResources*, *6*(4), 4200–4217.

Eronen, P., Laine, J., Ruokolainen, J., & Österberg, M. (2012). Comparison of multilayer formation between different cellulose nanofibrils and cationic polymers. *Journal of Colloid and Interface Science*, *373*(1), 84–93.

García-Ochoa, F., Santos, V. E., Casas, J. A., & Gómez, E. (2000). Xanthan gum: Production, recovery, and properties. *Biotechnology Advances*, *18*(7), 549–579.

Giri, M., Simonsen, J., & Rochefort, W. E. (2000). Dispersion of pulp slurries using carboxymethylcellulose. *Tappi Journal*, *October*, 1–14.

Gondo, T., Watanabe, M., Soma, H., & Kitao, O. (2006). SEC-MALS study on carboxymethyl cellulose (CMC): Relationship between conformation of CMC molecules and their adsorption behavior onto pulp fibers. *Nordic Pulp & Paper Research Journal*, *21*(5), 591–597.

Gregory, J., & Barany, S. (2011). Adsorption and flocculation by polymers and polymer mixtures. *Advances in Colloid and Interface Science*, *169*(1), 1–12.

Höök, F., Rodahl, M., Brzezinski, P., & Kasemo, B. (1998). Energy dissipation kinetics for protein and antibody–antigen adsorption under shear oscillation on a quartz crystal microbalance. *Langmuir*, *14*(4), 729–734.

Horvath, A. E., & Lindström, T. (2007). The influence of colloidal interactions on fiber network strength. *Journal of Colloidal and Interface Science*, *309*, 511–517.

Hubbe, M. A., & Rojas, O. J. (2008). Colloidal stability and aggregation of lignocellulosic materials in aqueous suspension: A review. *BioResources*, *3*(4), 1419–1491.

Iotti, M., Gregersen, O. W., Moe, S., & Lenes, M. (2011). Rheological studies of microfibrillar cellulose water dispersions. *Journal of Polymers and the Environment*, *19*(1), 137–145.

Junka, K., Filpponen, I., Johansson, L., Kontturi, E., Rojas, O. J., & Laine, J. (2012). A method for the heterogeneous modification of nanofibrillar cellulose in aqueous media. *Carbohydrate Polymers*, http://dx.doi.org/10.1016/j.carbpol.2012.11.063

Kang, K., Lettinga, M. P., Dogic, Z., & Dhont, J. K. G. (2006). Vorticity banding in rodlike virus suspensions. *Physical Review E*, *74*, 023607-1–026307-12.

Karppinen, A., Saarinen, T., Salmela, J., Laukkanen, A., Nuopponen, M., & Seppälä, J. (2012). Flocculation of microfibrillated cellulose in shear flow. *Cellulose*, *19*(6), 1807–1819.

Kasai, C., Namekawa, K., Koyano, A., & Omoto, R. (1985). Real-time two-dimensional blood flow imaging using an autocorrelation technique. *IEEE Transactions on Sonics and Ultrasonics*, *32*(3), 458–464.

Kerekes, R. J. (2006). Rheology of fibre suspensions in papermaking: An overview of recent research. *Nordic Pulp & Paper Research Journal*, *21*(5), 598–612.

Kerekes, R. J., Soszynski, R. M., & Tam Doo, P. A. (1985). The flocculation of pulp fibres. In *Transactions of the 8th Fundamental Research Symposium* (pp. 265–310).

Laine, J., Lindström, T., Nordmark, G. G., & Risinger, G. (2000). Studies on topochemical modification of cellulosic fibers. Part 1. Chemical conditions for the attachment of carboxymethyl cellulose onto fibers. *Nordic Pulp & Paper Research Journal*, *15*(5), 520–526.

Lee, P. F. W., & Lindström, T. (1989). Effects of high molecular mass anionic polymers on paper sheet formation. *Nordic Pulp & Paper Research Journal*, (2), 61–70.

Liimatainen, H., Haavisto, S., Haapala, A., & Niinimäki, J. (2009). Influence of adsorbed and dissolved carboxymethyl cellulose on fibre suspension dispersing, dewaterability, and fines retention. *BioResources*, *4*(1), 321–340.

Myllytie, P., Holappa, S., Paltakari, J., & Laine, J. (2009). Effect of polymers on aggregation of cellulose fibrils and its implication on strength development in wet paper web. *Nordic Pulp & Paper Research Journal*, *24*(2), 125–134.

Myllytie, P., Salmi, J., & Laine, J. (2009). The influence of pH on the adsorption and interaction of chitosan with cellulose. *BioResources*, *4*(4), 1647–1662.

Nguyen, D. L., Pahimanolis, N., Hippi, U., Korhonen, J. T., Ruokolainen, J., Johansson, L., et al. (2011). Graphene/cellulose nanocomposite paper with high electrical and mechanical performances. *Journal of Materials Chemistry*, *21*(36), 13991–13998.

Norton, I. T., & Goodall, D. M. (1984). Mechanism and dynamics of conformational ordering in xanthan polysaccharide. *Journal of Molecular Biology*, *175*, 371–394.

Orelma, H., Teerinen, T., Johansson, L., Holappa, S., & Laine, J. (2012). CMC-modified cellulose biointerface for antibody conjugation. *Biomacromolecules*, *13*(4), 1051–1058.

Pääkkö, M., Ankerfors, M., Kosonen, H., Nykänen, A., Ahola, S., Österberg, M., et al. (2007). Enzymatic hydrolysis combined with mechanical shearing and high-pressure homogenization for nanoscale cellulose fibrils and strong gels. *Biomacromolecules*, *8*(6), 1934–1941.

Rantanen, M., Molarius, S., Pikkarainen, S., Knuutinen, J., & Pakarinen, P. (2006). Effect of carboxymethyl cellulose on pulp dispersing. *Paperi Ja Puu – Paper and Timber*, *88*(6), 346–350.

Rochefort, W. E., & Middleman, S. (1987). Rheology of xanthan gum: Salt, temperature, and strain effects in oscillatory and steady shear experiments. *Journal of Rheology*, *31*(4), 337–369.

Rodahl, M., & Kasemo, B. (1996). On the measurement of thin liquid overlayers with the quartz-crystal microbalance. *Sensors and Actuators A: Physical*, *54*(1–3), 448–456.

Rodahl, M., Hook, F., Krozer, A., Brzezinski, P., & Kasemo, B. (1995). Quartz crystal microbalance setup for frequency and Q-factor measurements in gaseous and liquid environments. *Review of Scientific Instruments*, *66*(7), 3924–3930.

Saarinen, T., Haavisto, S., Sorvari, A., Salmela, J., & Seppälä, J. (2014). The effect of wall depletion on the rheology of microfibrillated cellulose water suspensions by optical coherence tomography. *Cellulose*, http://dx.doi.org/10.1007/s10570-014-0187-5

Saito, T., Nishiyama, Y., Putaux, J., Vignon, M., & Isogai, A. (2006). Homogeneous suspensions of individualized microfibrils from TEMPO-catalyzed oxidation of native cellulose. *Biomacromolecules*, *7*(6), 1687–1691.

Salmela, J., & Kataja, M. (2005). Floc rupture and re-flocculation in turbulent shear flow. In *Proceedings of Advances in Paper Science and Technology 13th Fundamental Research Symposium* Cambridge, 11–16 September.

Sauerbrey, G. (1959). The use of quartz oscillators for weighing thin layers and for microweighing. *Zeitschrift Für Physik*, *155*(2), 206–222.

Soszynski, R. M., & Kerekes, R. J. (1988). Elastic interlocking of nylon fibers suspended in liquid, Part 1. Nature of cohesion among fibers. *Nordic Pulp & Paper Research Journal*, (4), 172–179.

Stenius, P. (2000). Macromolecular, surface, and colloid chemistry. In P. Stenius (Ed.), *Forest products chemistry* (1st ed., pp. 170–276). Fapet Oy: Jyväskylä.

Svagan, A. J., Samir, M. A. S. A., & Berglund, L. A. (2007). Biomimetic polysaccharide nanocomposites of high cellulose content and high toughness. *Biomacromolecules*, *8*(8), 2556–2563.

Svedberg, A. (2012). *Improvement of the retention–formation relationship using three-component retention aid systems* (Ph.D. thesis). Sweden: Royal Institute of Technology.

Swerin, A., Ödberg, L., & Lindström, T. (1990). Deswelling of hardwood kraft pulp fibers by cationic polymers. *Nordic Pulp & Paper Research Journal*, *5*(4), 188–196.

Turbak, A. F., Snyder, F. W., & Sandberg, K. R. (1983). Microfibrillated cellulose, a new cellulose product: Properties, uses, and commercial potential. *Journal of Applied Polymer Science: Applied Polymer Symposium*, *37*, 815–827 (Proc. Cellul. Conf., 9th, 1982, Part 2).

Vartiainen, J., Pöhler, T., Sirola, K., Pylkkänen, L., Alenius, H., Hokkinen, J., et al. (2011). Health and environmental safety aspects of friction grinding and spray drying of microfibrillated cellulose. *Cellulose*, *18*(3), 775–786.

Verwey, E. J. W., & Overbeek, J. T. G. (1948). *Theory of the stability of lyophobic colloids*.

Watanabe, M., Gondo, T., & Kitao, O. (2004). Advanced wet-end system with carboxymethyl-cellulose. *Tappi Journal*, *3*(5), 15–19.

Weissenberg, K. (1947). A continuum theory of rheological phenomena. *Nature*, *159*(4035), 310–311.

Yan, H., Lindström, T., & Christiernin, M. (2006). Some ways to decrease fibre suspension flocculation and improve sheet formation. *Nordic Pulp & Paper Research Journal*, *21*(1), 36–43.

Yano, H., & Nakahara, S. (2004). Bio-composites produced from plant microfiber bundles with a nanometer unit web-like network. *Journal of Materials Science*, *39*(5), 1635–1638.

Yano, H., Sugiyama, J., Nakagaito, A. N., Nogi, M., Matsuura, T., Hikita, M., et al. (2005). Optically transparent composites reinforced with networks of bacterial nanofibers. *Advanced Materials*, *17*(2), 153–155.

Zauscher, S., & Klingenberg, D. J. (2000). Surface and friction forces between cellulose surfaces measured with colloidal probe microscopy. *Nordic Pulp & Paper Research Journal*, *15*(5), 459–468.

Zauscher, S., & Klingenberg, D. J. (2001). Friction between cellulose surfaces measured with colloidal probe microscopy. *Colloids and Surfaces A: Physicochemical and Engineering Aspects*, *178*(1–3), 213–229.

Zhao, R. H., & Kerekes, R. J. (1993). The effect of suspending liquid viscosity on fiber flocculation. *Tappi Journal*, *76*(2), 183–188.